Published in final edited form as:
Toxicol Appl Pharmacol. 2009 February 1; 234(3): 361–369. doi:10.1016/j.taap.2008.10.009.

Evaluation of ovotoxicity induced by 7, 12-dimethylbenz[a] anthracene and its 3,4-diol metabolite utilizing a rat *in vitro* ovarian culture system

Yoshiyuki Igawa[1,2], **Aileen F. Keating**[1,*], **Kathila S. Rajapaksa**[1,3], **I. Glenn Sipes**[4], and **Patricia B. Hoyer**[1]

1 *Department of Physiology, University of Arizona, Tucson, AZ 85745*

2 *BioPharma Center, Asubio Pharma Co., Ltd., Gunma, Japan*

3 *Amgen Inc., Toxicology Department, Thousand Oaks, CA, 91320-1799*

4 *Department of Pharmacology, University of Arizona, Tucson, AZ 85745*

Abstract

The polycyclic aromatic hydrocarbon 7, 12-dimethylbenz[a]anthracene, (DMBA), targets and destroys all follicle types in rat and mouse ovaries. DMBA requires bioactivation to DMBA-3,4-diol-1,2-epoxide for ovotoxicity via formation of the intermediate, DMBA-3,4-diol (catalyzed by microsomal epoxide hydrolase; mEH). mEH was shown to be involved in DMBA bioactivation for ovotoxicity induction in B6C3F$_1$ mouse ovaries. The current study compared DMBA and DMBA-3,4-diol mediated ovotoxicity, and investigated mEH involvement in DMBA-3,4-diol bioactivation in Fischer 344 (F344) rat ovary. F344 postnatal day (PND) 4 rat ovaries were cultured in vehicle control or media containing 1) DMBA or DMBA-3,4-diol (12.5 nM - 1 μM; 15 days); 2) DMBA (1μM; 6 h -15 days); and 3) DMBA (1μM) or DMBA-3,4-diol (75 nM) ± the mEH activity inhibitor cyclohexene oxide (CHO; 2 mM; 4 days). Ovaries were histologically evaluated and mEH mRNA and protein were measured by reverse transcriptase PCR or Western blotting, respectively. Ovotoxicity following 15 days of culture occurred ($P < 0.05$) at lower concentrations of DMBA-3,4-diol (12.5 nM - primordial; 75 nM - primary) than DMBA (75 nM - primordial; 375 nM - primary). The temporal pattern of mEH expression following DMBA exposure showed mRNA up-regulation ($P < 0.05$) on day 2, with increased protein ($P < 0.05$) on day 4, the earliest time of observed follicle loss ($P < 0.05$). mEH inhibition prevented DMBA-induced, but not DMBA-3,4-diol-induced ovotoxicity. These results demonstrate a conserved response in mice and rats for ovarian mEH involvement in DMBA bioactivation to its ovotoxic, 3,4-diol-1,2-epoxide form.

Keywords

Dimethylbenz[a]anthracene; ovotoxicity; microsomal epoxide hydrolase

*Corresponding author: Aileen F. Keating, University of Arizona, Department of Physiology, 1501 N. Campbell Ave., #4132, Tucson, Arizona 85724-5051, e-mail: akeating@email.arizona.edu, fax number: (520)626-2382, phone number: (520)626-5947.

Introduction

The ovary is a heterogeneous organ composed of follicles at various stages of growth. At birth the ovary contains a finite number of small preantral follicles (primordial and small primary), which can grow and mature toward ovulation. Since primordial follicles cannot be regenerated (Hirshfield, 1991), chemical-induced depletion of this follicle pool can lead to premature ovarian failure. This has been reported for a number of chemical exposures including the carcinogenic polycyclic aromatic hydrocarbon, 7,12-dimethylbenz[a]anthracene (DMBA; Mattison and Schulman, 1980; Hoyer *et al*., 2001). DMBA causes ovarian follicle disruption, targeting all follicle types, which ultimately results in premature ovarian failure in mice and rats (Mattison and Schulman, 1980). Sources of human exposure to DMBA are cigarette smoke, car exhaust fumes, and burning of organic matter (Gelboin, 1980).

Both the carcinogenic and ovotoxic properties of DMBA are attributed to its three-step bioactivation to a DMBA-3,4-diol-1,2-epoxide metabolite. DMBA is bioactivated in hepatic tissue by cytochrome P450 isoform 1B1 (CYP1B1) to a 3,4-epoxide, which is then hydrolyzed to a 3,4-diol by microsomal epoxide hydrolase (mEH; EC 3.3.2.3). This compound further undergoes epoxidation at the 1,2 position by CYP1A1 or CYP1B1 to form the ultimate carcinogen and ovotoxicant, DMBA-3,4-diol-1,2-epoxide (Figure 1; Miyata *et al*., 1999).

Several studies have shown that the mouse ovary expresses CYP1A1, CYP1B1 and mEH, and mRNA for these enzymes is inducible by xenobiotic exposures (Cannady *et al*., 2002; Shimada *et al*., 2003). A key role for ovarian mEH in DMBA bioactivation was shown in PND4 cultured $B6C3F_1$ neonatal mouse ovaries (Rajapaksa *et al*., 2007). This study utilized a whole ovary culture system that lacks metabolic input from the liver. Thus, all observed effects are ovarian specific (Devine *et al*., 2002). DMBA (at all concentrations studied) caused follicle loss via apoptosis, and increased expression of mEH mRNA preceded the follicle loss. Additionally, incubation of ovaries with the competitive inhibitor of mEH, cyclohexene oxide (CHO), prevented DMBA induced loss of primordial and small primary follicles (Rajapaksa *et al*., 2007). These findings supported that ovarian mEH is required for the bioactivation of DMBA to its ovotoxic form in mice. However, these studies did not investigate the possible involvement of mEH in ovotoxicity caused by intermediate DMBA metabolites such as DMBA-3,4-diol.

The current study investigated whether ovarian mEH in the rat ovary is also involved in DMBA-induced follicle loss. The hypothesis is that in the rat ovary, as with the mouse, mEH is involved in bioactivation of DMBA to its ovotoxic form. A neonatal rat whole ovarian culture system was used to investigate ovarian effects in the absence of the liver (Devine *et al*., 2002). Expression of mEH mRNA and protein were measured in response to DMBA exposure. Additionally, the role of mEH in metabolism of both DMBA and DMBA-3,4-diol to the active metabolite was determined using the DMBA-3,4-diol intermediate metabolite as well as inhibition of mEH activity using CHO.

Materials and Methods

Reagents

2-β-mercaptoethanol, 30% acrylamide/0.8% bis-acrylamide, ammonium persulfate, glycerol, N′,N′,N′,N′-Tetramethyl-ethylenediamine (TEMED), Tris base, TrisHCL, sodium chloride, Tween-20, bovine serum albumin (BSA), ascorbic acid (Vitamin C), 7,12-dimethylbenz [a] anthracene (DMBA; CAS # 57-97-6; 95% purity), cyclohexene oxide (CHO) and transferrin were purchased from Sigma-Aldrich Inc. (St Louis, MO). DMBA-3,4-diol (CAS # 72617-60-8; 98% purity) was purchased from the NCI Chemical Carcinogen Repository (Bethesda, MD). Dulbecco's Modified Eagle Medium: nutrient mixture F-12 (Ham) 1X (DMEM/Ham's F12),

Albumax, penicillin/streptomycin (5000U/ml, 5000mg/ml, respectively), Hanks' Balanced Salt Solution (without $CaCl_2$, $MgCl_2$, or $MgSO_4$), custom designed primers and Superscript III One-Step RT-PCR System were purchased from Invitrogen Co. (Carlsbad, CA). Millicell-CM filter inserts were purchased from Millipore (Bedford, MA), and 48 well cell culture plates were purchased from Corning Inc. (Corning, NY). RNeasy Mini kit, QIAshredder kit, RNeasy MinElute kit, and QuantitectTM SYBR Green PCR kit were purchased from Qiagen Inc. (Valencia, CA). RNAlater was obtained from Ambion Inc. (Austin, TX). The polyclonal mEH primary antibody (goat anti-rabbit) was purchased from Detroit R and D (Detroit, MI). Secondary antibody for anti-mEH (donkey anti-goat) was purchased from Vector (Burlingame, CA). The polyclonal β-actin primary antibody (mouse anti-rabbit) was purchased from Santa Cruz Biotechnology, CA). Goat anti-rabbit secondary antibody for anti-β-actin was obtained from Pierce Biotechnology (Rockford, IL). Cy-5-streptavidin was obtained from Vector (Burlingame, CA). YOYO-1 was purchased from Molecular Probes (Eugene, OR). ECL plus chemiluminescence detection kit was purchased from GE Healthcare, Amersham (Buckinghamshire, UK).

Animals

Late gestation day 18 pregnant Fischer 344 (F344) rats were purchased from Harlan Laboratories (Indianapolis, IN). All animals were housed one per cage in plastic cages, and maintained in a controlled environment (22 ± 2°C; 12h light/12h dark cycles). The animals were provided with a standard diet (Teklad 4% protein) with ad libidum access to food and water, and allowed to give birth. All animal experimental procedures were approved by the University of Arizona's Institutional Animal Care and Use Committee.

In vitro ovarian cultures

Culturing of ovarian tissue *in vitro* was performed as described in Parrott and Skinner (1999) with some modifications. Postnatal day (PND) 4 female Fischer 344 rats were euthanized by CO_2 inhalation followed by decapitation. Each ovary was removed, oviduct and excess tissue trimmed, and placed on a piece of Millicell-CM membrane floating on 250 μl of DMEM/Ham's F12 medium containing 1 mg/ml BSA, 1 mg/ml Albumax, 50 μg/ml ascorbic acid, 5 U/ml penicillin/5 μg/ml streptomycin, and 27.5 mg/ml transferrin in a well in a 48 well plate previously equilibrated to 37°C for at least 1 h. Using fine forceps a drop of medium was placed to cover the top of the ovary to prevent drying. Ovaries were incubated with 1% DMSO (vehicle control), DMBA, DMBA-3,4-diol, and/or CHO at concentrations indicated in figure legends. Concentrations of reagents were adapted from Rajapaksa *et al*. (2007). Plates containing ovaries were cultured at 37°C and 5% CO_2 in air. For those cultures lasting more than 2 days, media were removed and fresh media and treatment were added every 2 days.

Histological evaluation of follicle numbers

Following incubation, ovaries were placed in Bouin's fixative for 1.5 h, transferred to 70% ethanol, embedded in paraffin, serially sectioned (5 μm thick), and every 6^{th} section was mounted on the slide. All ovarian sections were stained with hematoxylin and eosin. NOTE: in cultured ovaries, follicles undergoing atresia are not readily cleared due to lack of circulating macrophages. Thus, following incubation, ovaries contain substantial amounts of healthy and unhealthy follicles and only healthy appearing follicles are counted (Rajapaksa *et al*., 2007). Healthy follicle populations containing oocytes were classified and counted in every 12^{th} section. Unhealthy follicles were distinguished from healthy follicles by pyknosis of granulosa cells and intense eosinophilic staining of oocytes (Devine *et al*., 2002). Follicle population classification was according to the procedure of Flaws *et al*. (1994) which was adapted from that described by Pedersen and Peters (1968). Briefly, primordial follicles contained the oocyte surrounded by a single layer of squamous-shaped granulosa cells; primary follicles contained

the oocyte surrounded by a single layer of cuboidal-shaped granulosa cells; secondary follicles contained the oocyte surrounded by multiple layers of granulosa cells; and antral follicles are identified by the fluid filled cavity (antrum) within the follicle. Follicle populations in the PND4 cultured ovary are mostly primordial and primary, with larger primary and secondary follicles developing after 4 days in culture (Devine *et al*., 2004).

RNA isolation and real-time polymerase chain reaction (PCR)

Following 1, 2 or 4 days of *in vitro* culture, ovaries (8/pool) treated with vehicle control (1% DMSO) or DMBA (1μM) were stored in RNAlater at −80°C. Total RNA was isolated using an RNeasy Mini kit. Briefly, ovaries were lysed and homogenized using a motor and pestle and the mixture was applied onto a QIAshredder column, followed by centrifugation at 14,000 rpm for 2 min. The resulting supernatant was applied to an RNeasy mini column, allowing RNA to bind to the filter cartridge. Following washing, RNA was eluted from the filter, and concentrated using an RNeasy MinElute kit. Briefly, isolated RNA was applied to an RNeasy MinElute spin column, and after washing, RNA was eluted using 14 μL of RNase-free water. RNA concentration was determined using a NanoDrop (λ= 260/280 nm; ND 1000; Nanodrop Technologies Inc., Wilmington, DE). Total RNA (1 μg) was reverse transcribed into cDNA utilizing the Superscript III One-Step RT-PCR System. Diluted cDNA (1:10; 2μL) were amplified on a Rotor-Gene 3000 using QuantitectTM SYBR Green PCR kit and custom designed primers for rat mEH (forward primer: 5′ GGC ATC ATG GTC CAT AAA CA 3′; reverse primer: 5′ TCT TCA AAG GCA GCA AAG TG; NCBI Genbank accession number M26125) and rat ribosomal protein L19 (forward primer: 5′ CGT CCT CCG CTG TGG TAA AAA G 3′; reverse primer: 5′ TTC GCA TCC AGG TCA CCT TCT C 3′; NCBI Genbank accession number NM 031103, Springer *et al*., 1996). The regular cycling program consisted of a 15 min hold at 95°C and 45 cycles of: denaturing at 95°C for 15 s, annealing at 58°C for 15 s, and extension at 72°C for 20 s at which point data were acquired. Product melt conditions were determined using a temperature gradient from 72°C to 99°C with a 1°C increase at each step. There was no difference in L19 mRNA between vehicle control and DMBA treated ovaries. Therefore, each sample was normalized to L19 before quantification.

Protein isolation and Western blot analysis

Following 2, 4 or 6 days of *in vitro* culture, ovaries (8/pool) treated with vehicle control (1% DMSO) or DMBA (1 μM) were frozen in liquid nitrogen and stored at −80°C. Pools of whole ovarian protein homogenates were prepared from cultured ovaries via homogenization in tissue lysis buffer as previously described (Thompson *et al*., 2005). Briefly, homogenized samples were placed on ice for 30 min, followed by two rounds of centrifugation at 10,000 rpm for 15 min. Supernatant was aliquoted and stored at −80°C until further use. Protein was quantified using a standard BCA protocol on a 96-well assay plate. Emission absorbance values were detected with a λ =540 nm excitation on a Synergy™ HT Multi-Detection Microplate Reader using KC4™ software (BioTek® Instruments Inc. Winooski, VT). Protein concentrations were calculated from a BSA protein standard curve.

SDS-PAGE (12%) was used to separate protein homogenates (10 or 20 μg; n=3) and subsequently transferred onto nitrocellulose membranes as previously described (Thompson *et al*., 2005). Briefly, membranes were blocked for 1 h with shaking at 4°C in 5% milk in Tris-buffered saline with Tween-20 (TTBS). Membranes were incubated with primary antibody in 5% milk in TTBS overnight at 4°C. Antibody dilutions used were mEH (1:10,000) and β-actin (1:1000). Membranes were washed three times for 10 min each with TTBS. HRP-conjugated secondary antibody (1:2000 dilution) was added for 1 h at room temperature. Membranes were washed three times for 10 min each in TTBS, followed by a single wash for 10 min in Tris Buffered Saline (TBS). Western blots were detected by chemiluminescence (using ECL plus chemiluminescence detection substrate) and exposed to X-ray film. Densitometry of the

appropriate bands was perfomed using LabWorks™ software from a UVP Bioimaging system (UVP Inc., Upland, CA). Individual treatment values were normalized to β-actin.

Confocal microscopy

Following 4 days of *in vitro* culture, ovaries treated with vehicle control (1% DMSO) or DMBA (1μM) were fixed in 4% buffered formalin for 2 h, transferred to 70% ethanol, embedded in paraffin, serially sectioned, and every 10th section was mounted. Sections were deparaffinized (10 sections/ovary) and incubated with the mEH primary antibody (goat anti-rabbit; 1:50 dilution) at 4°C overnight. Secondary biotinylated antibody (horse anti-goat; 1:75 dilution) was applied for 1 h, followed by CY-5-streptavidin (1 h; 1:50 dilution). Sections were treated with Ribonuclease A (100 mg/ml) for 1 h, followed by staining with YOYO-1 (10 min; 5 nM). Slides were repeatedly rinsed with phosphate buffer saline (PBS), cover-slipped, and stored in the dark (4°C) until visualization. Primary antibody was not added to immunonegative ovarian sections. Immunofluorescence was visualized on a Zeiss (LSM 510 NLO-Meta) confocal microscope with an argon and helium-neon laser projected through the tissue into a photomultiplier at l = 488 and 633 nm for YOYO-1 (green) and CY-5 (red), respectively. All images were captured using a 40X objective lens.

Statistical analysis

Comparisons were made using one-way ANOVA. When significant differences were detected, individual groups were compared with the Fisher's protected least significant difference (PLSD) multiple range test. The assigned level of significance for all tests was $P < 0.05$.

Results

Evaluation of DMBA-Induced Follicle Loss

Follicle loss was evaluated in PND4 rat ovaries following 15 days of incubation with increasing concentrations (12.5 nM - 1 μM) of DMBA (Figure 2). Compared to vehicle control, DMBA reduced ($P < 0.05$) healthy primordial follicles at concentrations ≥75 nM (Figure 2A). Healthy primary follicles were reduced ($P < 0.05$) at concentrations ≥375 nM DMBA (Figure 2B). Essentially all healthy follicle populations were depleted by DMBA at concentrations ≥750 nM.

Evaluation of DMBA-3,4-diol-Induced Follicle Loss

Follicle loss was evaluated in PND4 rat ovaries following 15 days of incubation with increasing concentrations (12.5 nM - 1 μM) of the intermediate metabolite DMBA-3,4-diol (Figure 3). Compared to vehicle control, DMBA-3,4-diol reduced ($P < 0.05$) healthy primordial follicles at 12.5 nM (Figure 3A). Concentrations ≥75 nM DMBAwere required to reduce the number of healthy primary follicles ($P < 0.05$; Figure 3B). Essentially all healthy follicle populations were depleted by DMBA at concentrations of ≥250 nM.

Time Course of DMBA-Induced Follicle Loss

Follicle loss was evaluated in PND4 rat ovaries incubated with 1 μM DMBA for various time points (6 h - 15 days; Figure 4). Relative to vehicle control, ovaries incubated with DMBA for 4 days showed primordial and primary follicle loss ($P < 0.05$). All healthy primordial and primary follicles were depleted in these ovaries by 12 days of culture (Figure 4A and 4B).

Effect of mEH Inhibition on DMBA- or DMBA-3,4-Diol-Induced Follicle Loss

Follicle loss was evaluated in PND4 rat ovaries following 4 days of incubation with an mEH enzyme inhibitor, cyclohexene oxide (CHO, Figure 5). Incubations with CHO (2 mM) alone did not affect total follicle populations. DMBA (1 μM) decreased ($P < 0.05$) total follicles

following 4 days in culture, and CHO prevented the loss of follicles induced by DMBA (Figure 5A). Conversely, whereas the intermediate metabolite DMBA-3,4-diol (75 nM) decreased ($P < 0.05$) healthy follicles relative to control, inclusion of CHO did not prevent DMBA-3, 4-diol-induced follicle loss (Figure 5B).

Effect of DMBA on Ovarian Expression of mRNA encoding mEH

To investigate the effect of DMBA on ovarian mEH enzyme expression, the level of mRNA encoding mEH in ovaries collected from PND4 rats following DMBA treatment was quantified using real-time PCR. Following incubation with 1 μM DMBA for 1 day, mRNA encoding mEH was unchanged compared to that of the vehicle control group. At 2 and 4 days of DMBA exposure, there were 32 and 69 % increases ($P < 0.05$) in mRNA encoding mEH compared to vehicle control, respectively (Figure 6).

Effect of DMBA on Ovarian Expression of mEH Protein

To further evaluate the effect of DMBA on ovarian mEH, the level of mEH protein in ovaries collected from PND4 rats following DMBA treatment was quantified by Western blot analysis. Following incubation with 1 μM DMBA for 2, 4 and 6 days, mEH protein increased ($P < 0.05$) by 119, 148, and 116 % compared to vehicle control groups, respectively (Figure 7). Furthermore, to visualize protein expression, confocal microscopy analysis was conducted using ovaries treated with vehicle control or 1 μM DMBA for 4 days. mEH protein was highly localized to the cytoplasm of both oocytes and granulosa cells. Following incubation with 1 μM DMBA, staining intensity of mEH protein in the cytoplasm of follicles was elevated compared with ovaries incubated with vehicle control (Figure 8).

Discussion

DMBA, a potent carcinogen, causes destruction of all follicle types in the ovary (Mattison, 1980; Weitzman *et al*., 1992). It requires a series of metabolic reactions to form the ovotoxic metabolite, DMBA-3,4-diol-1,2-epoxide in order to mediate its carcinogenic and ovotoxic effects (Shiromizu and Mattison, 1985, Vigny *et al*., 1985). In vivo studies in mice have shown the intermediate, DMBA-3,4-diol, to be a more potent ovotoxicant than the parent compound (Matikainen *et al*., 2001). The sequential steps for DMBA bioactivation are catalyzed by CYP1B1, mEH and CYP1A1/CYP1B1, respectively, to form DMBA-3,4-diol-1,2-epoxide (Figure 1). These enzymes (CYP1B1, CYP1A1 and mEH) have been shown to be expressed by the ovary (Shimada *et al*., 2003; Cannady *et al*., 2002).

It has been demonstrated that DMBA-induced ovotoxicity in the $B6C3F_1$ PND4 neonatal mouse ovary is preceded by an increase in expression of mEH mRNA and protein. Additionally, DMBA-induced ovotoxicity was prevented when activity of mEH was inhibited (Rajapaksa *et al*., 2007). While it has been demonstrated that ovarian mEH bioactivates DMBA to an ovotoxic metabolite, no study has investigated the role of ovarian mEH in bioactivation of the DMBA-3,4-diol metabolite to DMBA-3,4-diol-1,2-epoxide. Because DMBA-3,4-diol is an intermediate in the conversion of DMBA to the ovotoxic DMBA-3,4-diol-1,2-epoxide, incubation with this metabolite should be more directly ovotoxic and thus be more potent in terms of ovotoxicity than DMBA. Thus, the current study investigated the role of ovarian mEH in DMBA-induced ovotoxicity in the PND4 neonatal F344 rat ovary. The metabolic role of the liver was eliminated by using a whole neonatal rat ovarian culture method, therefore, all effects seen were the result of ovarian function.

Relative to control treatments, DMBA exposure resulted in primordial (≥75 nM DMBA) and small primary (≥375 nM DMBA) follicle loss. In contrast, much lower concentrations of the 3,4-diol intermediate metabolite were effective at causing this follicle loss (≥12.5 nM

primordial follicle loss; ≥75 nM small primary loss). These results point to the importance of bioactivation to the active metabolite for induction of follicle loss. It is also interesting to note that lower concentrations of both chemicals were required for loss of primordial follicles than those required for small primary follicle loss. This suggests that either primordial follicles are more sensitive to the ovotoxic metabolite or that an increase in recruitment from the primordial to primary follicle pool during DMBA-induced follicle loss has occurred.

DMBA-induced primordial and small primary follicle loss was also observed in the $B6C3F_1$ PND4 neonatal cultured mouse ovary (Rajapaksa *et al*., 2007). However, in contrast to the rat ovary, lower concentrations of DMBA were effective at inducing a similar degree of ovotoxicity in the mouse ovary (primordial follicle loss: mouse - 12.5 nM, rat - 75 nM; small primary follicle loss: mouse - 25 nM, rat - 375 nM). Furthermore, at 1μM, DMBA-induced loss of both primordial and small primary follicles occurred after 6 hours, but after 4 days in the rat ovary. Thus, in terms of ovotoxicity, the $B6C3F_1$ mouse ovary is more sensitive to DMBA-induced follicle loss than the F344 rat ovary. This was also shown in an *in vivo* study where mice and rats were dosed daily with increasing concentrations of DMBA for 15 days. The DMBA concentration required to cause 50% primordial follicle loss was determined and shown that this concentration was 350-fold higher in rats than in mice (Borman *et al*., 2000). The reason for this species difference in susceptibility is not known at this time.

To more directly explore the role of ovarian mEH in DMBA bioactivation, mEH activity was inhibited using CHO. CHO acts as an alternative substrate for mEH, and competitively inhibits its activity. Thus, with CHO, metabolism of DMBA to DMBA-3,4-diol-1,2-epoxide (active metabolite) should be reduced (Oesch, 1973). Whereas DMBA (1 μM; 4 days) caused loss of primordial and small primary follicles, there was no follicle loss when CHO was included in DMBA-containing medium compared to control. Thus, inhibited bioactivation resulted in inhibited follicle loss. During bioactivation of DMBA, mEH activity produces the intermediate DMBA-3,4-diol. Because it is downstream of mEH, inhibition of mEH should not affect DMBA-3,4-diol-induced ovotoxicity. This was found to be the case. Unlike the ability of CHO to prevent DMBA-induced ovotoxicity, it had no effect on DMBA-3,4-diol. These results provide a direct functional demonstration of the importance of ovarian mEH in the bioactivation of DMBA to the ovotoxic DMBA-3,4-diol to induce ovotoxicity.

A number of other studies have shown the important role of DMBA bioactivation in its induction of toxicological effects. CYP1B1 null mice treated with DMBA were less susceptible to ovarian DMBA-induced DNA adduct formation in the ovary (Buters *et al*., 2003). mEH null mice treated with DMBA were more resistant to skin cancer than wild-type mice, and the active metabolite, DMBA-3,4-diol, was not detected in embryonic fibroblasts from DMBA-treated mEH null mice (Miyata *et al*., 1999).

DMBA-induced immunotoxicity in mEH null mice has been investigated (Gao *et al*., 2007). mEH wild type and null mice were orally gavaged with corn oil (vehicle control) or DMBA (0, 17, 50 and 150 mg/kg) once daily for five days. A plaque-forming cell assay (PFC) in response to sheep red blood cells (SRBC) was performed on spleen cells and demonstrated that, relative to control, there was no effect of DMBA on mEH null mice. In a previous study by these same authors, wild type mouse spleen cells were treated with T- and B-cell mitogens (Con A and LPS, respectively) and DMBA exposure resulted in suppression of the T- and B-cell response (Gao *et al*., 2005). When this study was performed in mEH null mice exposed to DMBA, there was no altered B-cell mitogen response and the T-cell response was different from the mEH wild type mice. Similarly, mEH null mice did not demonstrate a reduction in natural killer cell activity due to DMBA treatment as did the mEH wild type mice (Gao *et al*., 2007). Thus, collectively, these results support that mEH is critical for metabolism of

DMBA to the active DMBA-3,4-diol-1,2-epoxide metabolite for both carcinogenic and immunotoxic effects to occur.

To further examine its potential involvement in DMBA-induced ovotoxicity, ovarian mEH level was investigated in ovaries exposed to DMBA. A time-course of mEH expression was compared to the temporal pattern of DMBA-induced follicle loss. mEH mRNA and protein level were elevated by day 2, while follicle loss was observed on day 4. Thus, the increase in mEH preceded follicle loss. This finding further supports a role for ovarian mEH in bioactivation of DMBA to its ovotoxic form. Increased levels of mEH mRNA also preceded DMBA-induced follicle loss in $B6C3F_1$ mouse neonatal cultured ovaries (Rajapaksa *et al*., 2007). Interestingly in that study, an increase in follicle loss from 45 to 90% occurred just after an observed large increase (5.2-fold) in mEH mRNA level on day 2 pointing to an active involvement of ovarian mEH in bioactivation of DMBA (Rajapaksa *et al*., 2007). Thus, DMBA-induced follicle loss occurring subsequent to an increase in mEH mRNA is conserved between mice and rats.

The opposing roles of ovarian mEH in chemical bioactivation (Rajapaksa *et al*., 2007) and detoxification (Cannady *et al*., 2002; Keating *et al*., 2008a, b) have been demonstrated. 4-vinylcyclohexene (VCH) and its metabolites are examples of occupational chemicals that cause ovotoxicity. The diepoxide metabolite of VCH, VCD, has been shown to be the ultimate ovotoxicant in mice and rats, specifically targeting small pre-antral (primordial and primary) follicles (Doerr *et al*., 1995; Smith *et al*., 1990). Ovarian mEH is up-regulated in response to VCD exposure (Cannady *et al*., 2002, Keating *et al*., 2008a, b). This up-regulation results in less ovotoxicity because of the enhanced ovarian capacity to detoxify VCD by mEH.

The ovotoxic effects of VCD and DMBA were compared using an ovotoxic index (concentration required for 50% primordial follicle loss), and it was shown that DMBA was approximately 20 times more potent than VCD in terms of ovotoxicity (Borman *et al*., 2000). The differences in the ovotoxic effects of VCD and DMBA are likely contributed to by ovarian mEH. Because conversion of VCD to the tetrol is a detoxification reaction, mEH reduces the degree of ovotoxicity. However, in contrast, mEH bioactivates DMBA to a more toxic metabolite, and thus it accelerates follicle loss. The ovotoxic effects observed for these two chemicals underscore how the chemical nature of the metabolite produced by an ovarian enzyme dictates the toxic outcome.

Collectively, the results presented in this study highlight the role of mEH in the rat ovary and support that ovarian mEH is required for bioactivation of DMBA to the ovotoxic metabolite, DMBA-3,4-diol-1,2-epoxide. These results also demonstrate that this bioactivation involves formation of the intermediate metabolite, DMBA-3,4-diol, catalyzed by mEH. Additionally, induction of mEH by DMBA further enhances bioactivation and ovotoxicity of DMBA.

Acknowledgements

The authors wish to thank Andrea Grantham for histological processing of ovarian tissue and Patricia Christian for assistance with immunohistochemistry and confocal analysis.

This work was supported by National Institutes of Health grant ES09246 and Center Grant 06694.

Literature cited

Borman SM, Christian PJ, Sipes IG, Hoyer PB. Ovotoxicity in female Fisher rats and B6 mice induced by low-dose exposure to three polycyclic aromatic hydrocarbons: comparison through calculation of an ovotoxic index. Toxicol Appl Pharmacol 2000;167:191–198. [PubMed: 10986010]

Buters J, Qunitanilla-Martinez L, Schober W, Soballa VJ, Hintermair J, Wolff T, Gonzalez FJ, Greim H. CYP1B1 determines susceptibility to low doses of 7, 12-dimethylbenz[a]anthracene-induced ovarian cancers in mice: correlation of CYP1B1-mediated DNA adducts with carcinogenicity. Carcinogenesis 2003;24:327–334. [PubMed: 12584184]

Cannady EA, Dyer CA, Christian PJ, Sipes IG, Hoyer PB. Expression and activity of microsomal epoxide hydrolase in follicles isolated from mouse ovaries. Toxicol Sci 2002;68:24–31. [PubMed: 12075107]

Devine PJ, Sipes IG, Skinner MK, Hoyer PB. Characterization of a rat in vitro ovarian culture system to study the ovarian toxicant 4-vinylcyclohexene diepoxide. Toxicol Appl Pharmacol 2002;184:107–115. [PubMed: 12408955]

Devine PJ, Sipes IG, Hoyer PB. Initiation of delayed ovotoxicity by in vitro and in vivo exposure of rat ovaries to 4-vinylcyclohexene diepoxide. Reprod Toxicol 2004;19:71–77. [PubMed: 15336714]

Doerr JK, Hooser SB, Smith BJ, Sipes IG. Ovarian toxicity of 4-vinylcyclohexene and related olefins in B6C3F1 mice:role of diepoxides. Chem Res Toxicol 1995;8:963–969. [PubMed: 8555412]

Flaws JA, Doerr JK, Sipes IG, Hoyer PB. Destruction of preantral follicles in adult rats by 4-vinyl-1-cyclohexene diepoxide. Reprod Toxicol 1994;8:509–514. [PubMed: 7881202]

Gao J, Lauer FT, Dunaway S, Burchiel SW. cytochrome P450 1B1 is required for 7,12-dimethylbenz[a] anthracene (DMBA) induced spleen cell immunotoxicity. Toxicol Sci 2005;86:68–74. [PubMed: 15843505]

Gao J, Lauer FT, Mitchell LA, Burchiel SW. Microsomal epoxide hydrolase is required for 7,12-dimethylbenz[a]anthracene (DMBA)-induced immunotoxicity in mice. Toxicol Sci 2007;98:137–144. [PubMed: 17442664]

Gelboin HV. Benzo(*a*)pyrene metabolism, activation and carcinogenesis: role and regulation of mixed-function oxidases and related enzymes. Physiol Rev 1980;60:1107–66. [PubMed: 7001511]

Hirshfield AN. Development of follicles in the mammalian ovary. Int Rev Cytol 1991;124:43–101. [PubMed: 2001918]

Hoyer PB. Reproductive toxicology: current and future directions. Biochem Pharmacol 2001;62:1557–1564. [PubMed: 11755108]

Keating AF, Sipes IG, Hoyer PB. Expression of ovarian microsomal epoxide hydrolase and glutathione *S*-transferase during onset of VCD-induced ovotoxicity in B6C3F$_1$ mice. Toxicol Appl Pharmacol 2008a;230:109–16. [PubMed: 18407309]

Keating AF, Rajapaksa KS, Sipes IG, Hoyer PB. Effect of CYP2E1 gene deletion in mice on expression of microsomal epoxide hydrolase in response to VCD exposure. Toxicol Sci. 2008bIn Press

Matikainen T, Perez GI, Jurisicova A, Pru JK, Schlezinger JJ, Ryu H, Laine J, Sakai T, Korsmeyer S, Casper R, Sherr DH, Tilly JL. Aromatic hydrocarbon receptor-driven Bax gene expression is required for premature ovarian failure caused by biohazard environmental chemicals. Nat Genet 2001;28:355–360. [PubMed: 11455387]

Mattison DR, Schulman JD. How xenobiotic chemicals can destroy oocytes. Contemp Obstet Gynecol 1980;15:157.

Miyata M, Judo G, Lee Y, Yang TJ, Gelboni HV, Fernandez-Salguero P, Kimura S, Gonzalez FJ. Targeted disruption of the microsomal epoxide hydrolase gene. Microsomal epoxide hydrolase is required for the carcinogenic activity of 7,12-dimethylbenz[a]anthracene. J Biol Chem 1999;274:23963–23968. [PubMed: 10446164]

Oesch F. Mammalian epoxide hydrases: inducible enzymes catalyzing the inactivation of carcinogenic and cytotoxic metabolites derived from aromatic and olefinic compounds. Xenobiotica 1973;3:305–340. [PubMed: 4584115]

Parrott JA, Skinner MK. Kit-ligand/stem cell factor induces primordial follicle development and initiates folliculogenesis. Endocrinol 1999;140:4262–4271.

Pedersen T, Peters H. Proposal for a classification of oocytes and follicles in the mouse ovary. J Reprod Fertil 1968;17:555–557. [PubMed: 5715685]

Rajapaksa KS, Sipes IG, Hoyer PB. Involvement of microsomal epoxide hydrolase in ovotoxicity caused by 7,12-dimethylbenz[a]anthracene. Toxicol Sci 2007;96:327–334. [PubMed: 17204581]

Shimada T, Sugie A, Shindo M, Nakajima T, Azuma E, Hashimoto M, Inoue K. Tissue-specific induction of cytochromes P450 1A1 and 1B1 by polycyclic aromatic hydrocarbons and polychlorinated

biphenyls in engineered C57BL/6J mice of arylhydrocarbon receptor gene. Toxicol Appl Pharmacol 2003;187:1–10. [PubMed: 12628579]

Shiromizu K, Mattison DR. Murine oocyte destruction following intraovarian treatment with 3-methylcholanthrene or 7,12-dimethylbenz(a)anthracene: protection by alpha-naphthoflavone. Teratog Carcinog Mutagen 1985;5:463–72. [PubMed: 2874631]

Smith BJ, Mattison DR, Sipes IG. The role of epoxidation in 4-vinylcyclohexene-induced ovarian toxicity. Toxicol Appl Pharmacol 1990;105:372–381. [PubMed: 2237912]

Springer LN, Tilly JL, Sipes IG, Hoyer PB. Enhanced expression of bax in small preantral follicles during 4-vinylcyclohexene diepoxide-induced ovotoxicity in the rat. Toxicol Appl Pharmacol 1996;139:402–10. [PubMed: 8806858]

Thompson KE, Bourguet SM, Christian PJ, Benedict JC, Sipes IG, Flaws JA, Hoyer PB. Differences between rats and mice in the involvement of the aryl hydrocarbon receptor in 4-vinylcyclohexene diepoxide-induced ovarian follicle loss. Toxicol Appl Pharmacol 2005;203:114–123. [PubMed: 15710172]

Vigny P, Brunissen A, Phillips DH, Cooper CS, Hewer A, Grover PL, Sims P. Metabolic activation of 7,12-dimethylbenz[a]anthracene in rat mammary tissue: fluorescence spectral characteristics of hydrocarbon-DNA adducts. Cancer Lett 1985;26:51–59. [PubMed: 3918788]

Weitzman GA, Miller MM, London SN, Mattison DR. Morphometric assessment of the murine ovarian toxicity of 7,12-dimethylbenz[a]anthracene. Reprod Toxicol 1992;6:137–141. [PubMed: 1591471]

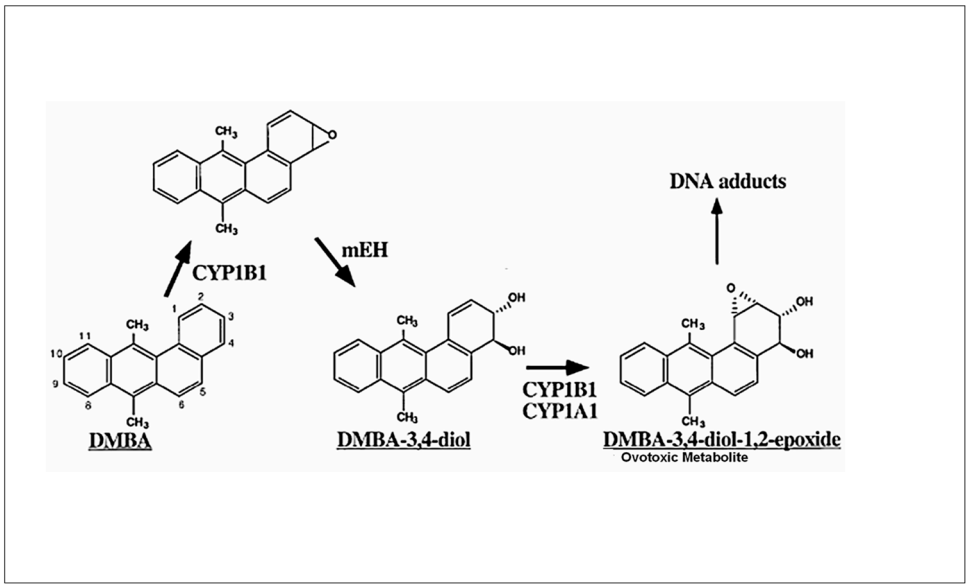

Figure 1. DMBA metabolic pathway

The parent compound, DMBA, is bioactivated by CYP450 isoform 1B1 (CYP1B1) to a DMBA-3, 4-epoxide intermediate, which is hydrolyzed by mEH to form DMBA-3,4-diol. This compound further undergoes bioactivation by either CYP1B1 or 1A1 to form the ultimate carcinogenic and ovotoxic metabolite, DMBA-3,4-diol-1,2-epoxide (Adapted from Miyata *et al*., 1999).

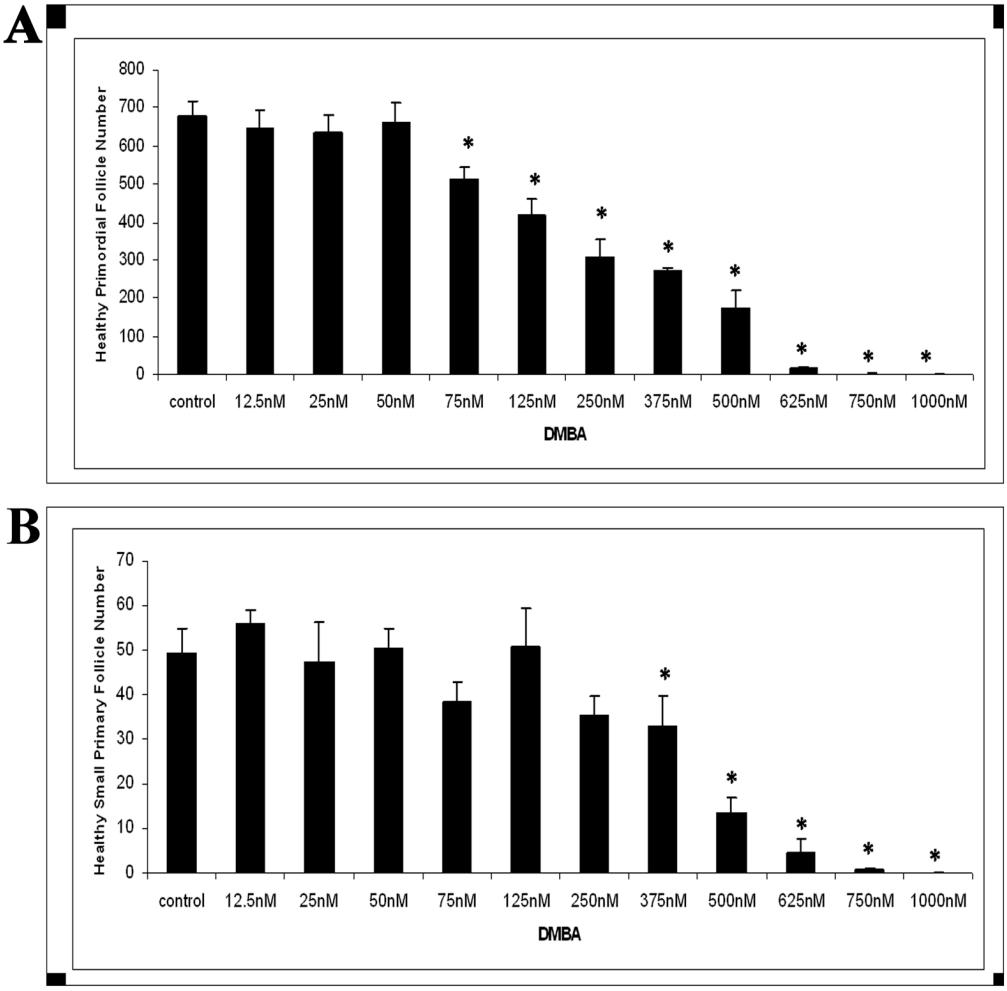

Figure 2. Effect of varying concentrations of DMBA on follicle numbers

Ovaries from PND4 Fischer 344 neonatal rats were cultured with vehicle control or DMBA (12.5 nM - 1 μM) for 15 days. Following incubation, ovaries were collected, and processed for histological evaluation as described in methods. Healthy (A) primordial and (B) primary follicles were classified and counted. Values are mean ± SE total follicles counted per ovary, n=5; * = different from each follicle type control, $P < 0.05$.

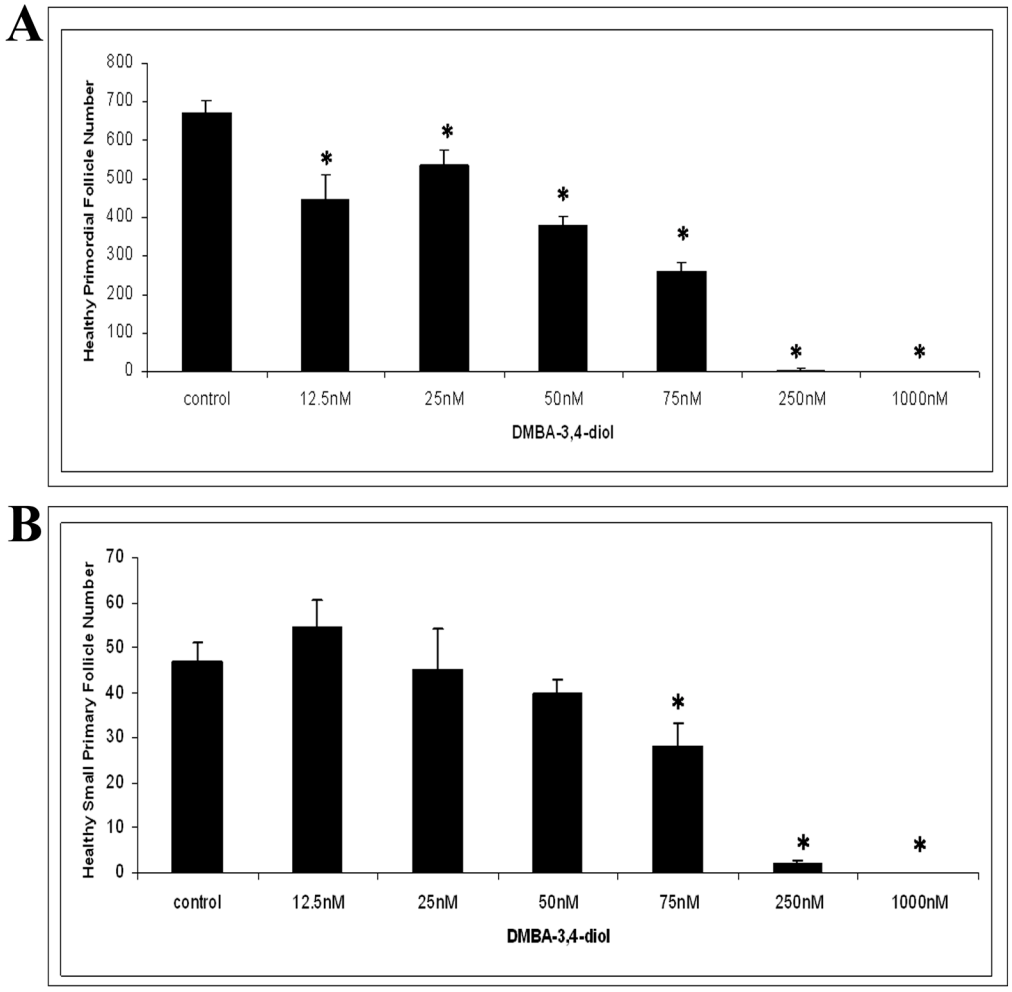

Figure 3. Effect of varying concentrations of DMBA-3,4-diol on follicle numbers

Ovaries from PND4 Fischer 344 neonatal rats were cultured with vehicle control or the intermediate metabolite DMBA-3,4-diol (12.5 nM - 1 μM) for 15 days. Following incubation, ovaries were collected, and processed for histological evaluation as described in methods. Healthy primordial (A) and primary (B) follicles were classified and counted. Values are mean ± SE total follicles counted per ovary, n=5; * = different from control in each follicle type, $P < 0.05$.

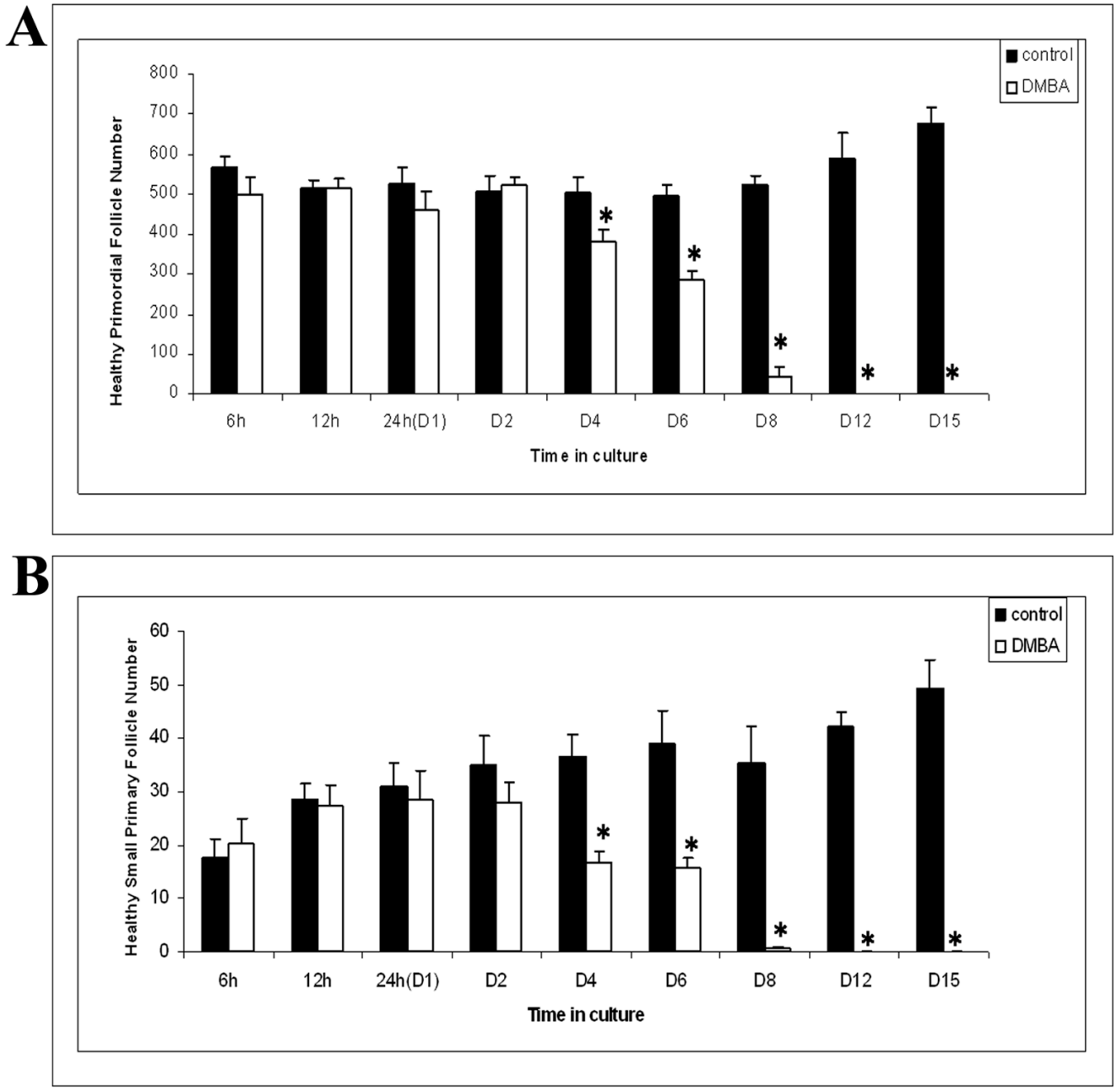

Figure 4. Time course of DMBA-induced follicle loss

Ovaries from PND4 Fischer 344 neonatal rats were cultured with vehicle control or 1 μM DMBA for 6 h - 15 days. Following incubation, ovaries were collected, and processed for histological evaluation. Healthy (A) primordial and (B) primary follicles were classified and counted. Values are mean ± SE total follicles counted per ovary, n=5; * = different from each follicle type control at each time point, $P < 0.05$.

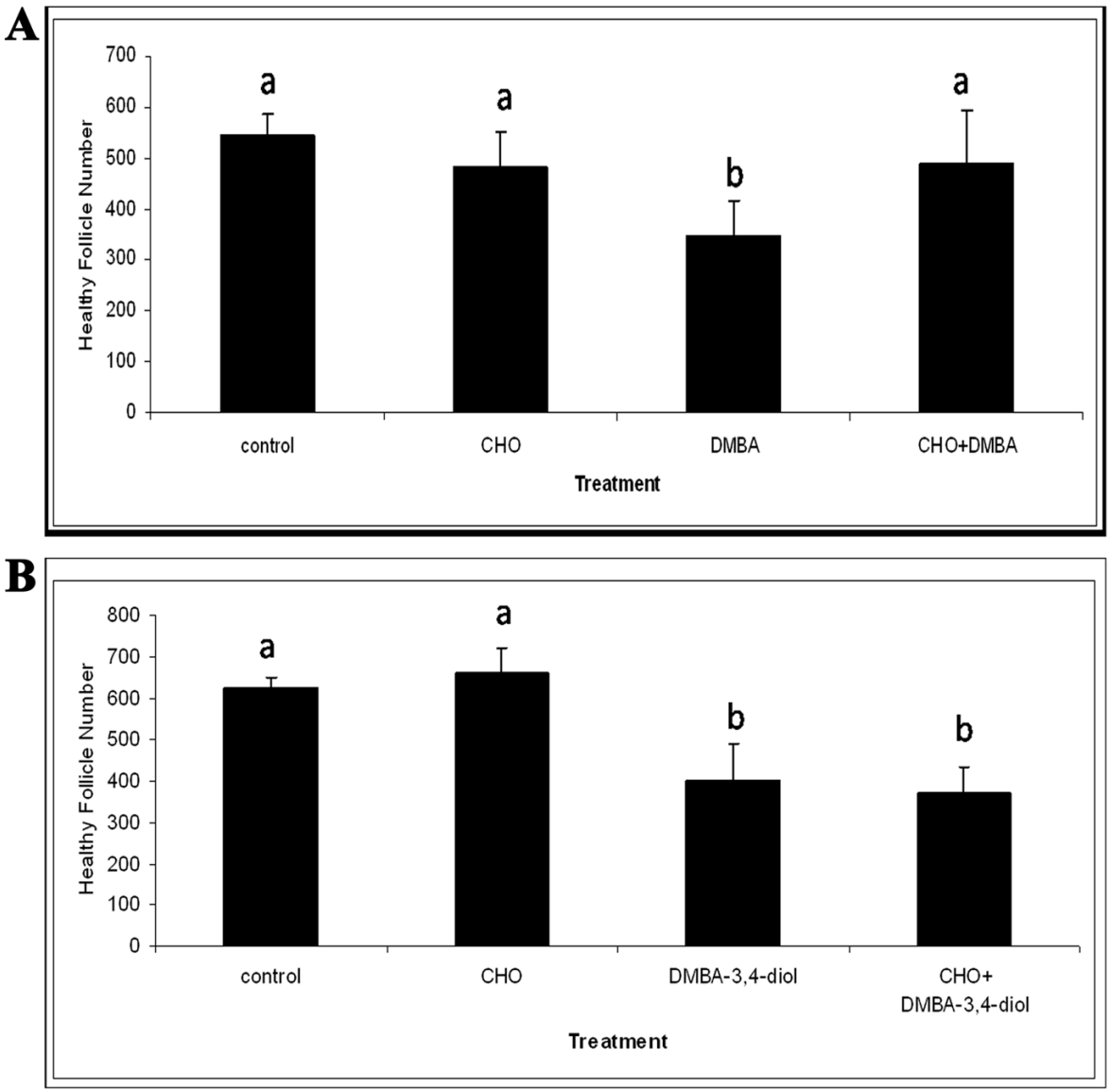

Figure 5. Effect of CHO (mEH inhibitor) on DMBA- or DMBA-3,4-diol-induced follicle loss

Ovaries from PND4 Fischer 344 rats were cultured with (A) vehicle control or media containing DMBA (1 μM) +/− CHO (2 mM) for 4 days; or (B) vehicle control or media containing DMBA-3,4-diol (75 nM) +/− CHO (2 mM) for 4 days. Following incubation, ovaries were collected, processed for histological evaluation and healthy follicles were counted as described in methods. Values are mean ± SE total follicles counted/ovary, n=5; * = different from control in each follicle type, $P < 0.05$.

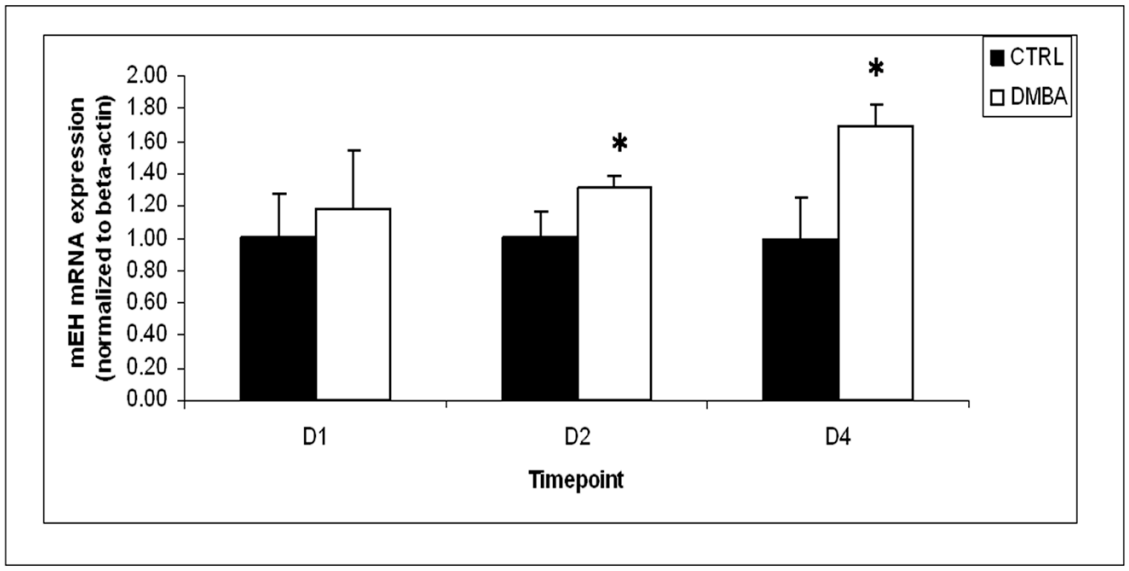

Figure 6. Effect of DMBA on mRNA encoding mEH

Ovaries from PND4 Fischer 344 neonatal rats were cultured with vehicle control or 1 μM DMBA for 1, 2 and 4 days. Following incubation, ovaries were collected and processed for measurement of mRNA encoding mEH by real-time PCR as described in methods. Values are mean ± SE expressed as ratio of treatment/control (8 ovaries/sample; n=3); * = different from control, $P < 0.05$.

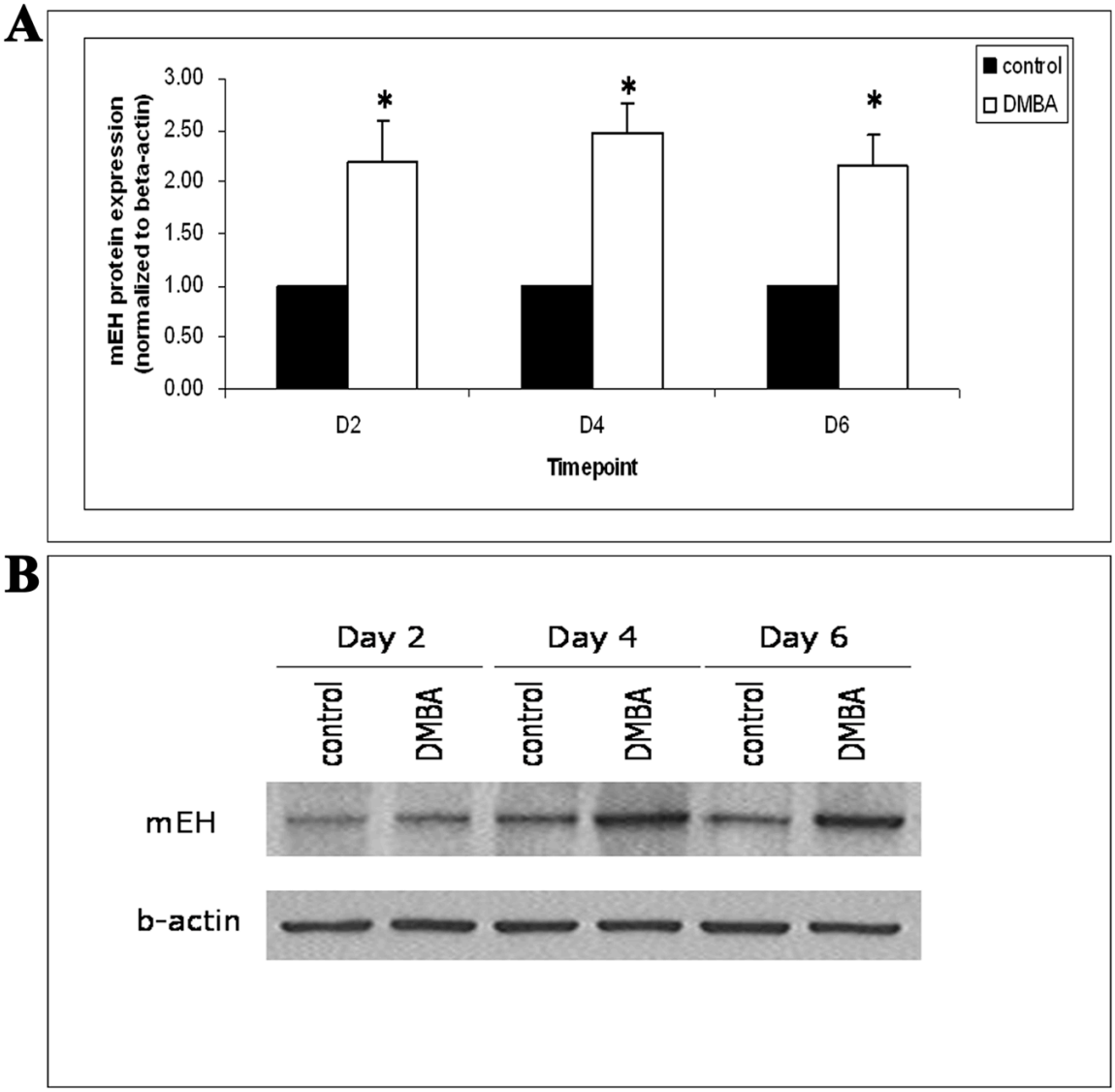

Figure 7. Effect of DMBA on mEH protein levels

Ovaries from PND4 Fischer 344 rats were cultured with vehicle control or 1 μM DMBA for 2, 4 and 6 days. Following incubation, ovaries were collected and processed for measurement of mEH protein by Western blot analysis as described in the Methods section. (A) Values are mean ± SE expressed as ratio of treatment/control (8 ovaries per sample; n=3); * = different from control, $P < 0.05$. (B) Representative Western blot gel using an anti-mEH antibody and anti-beta-actin antibody to confirm equal loading of samples.

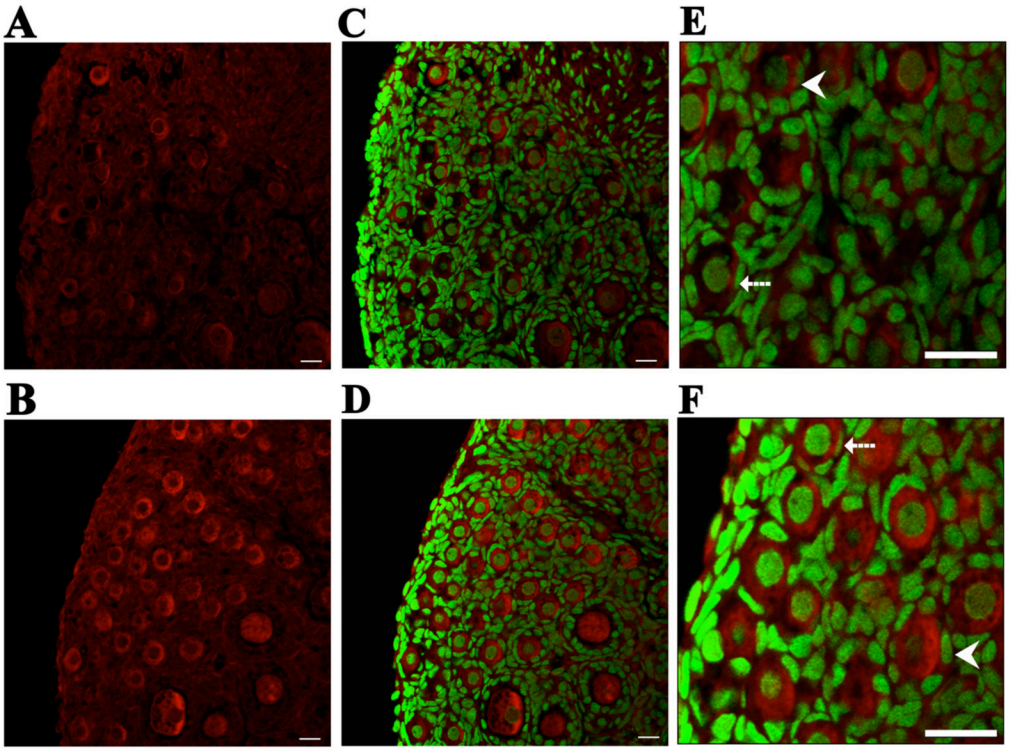

Figure 8. Effect of DMBA on visualization of mEH protein

Ovaries from PND4 Fischer 344 rats were cultured with vehicle control (A, C, E) or 1 μM DMBA (B, D, F) for 4 days. Following incubation, ovaries were processed for confocal microscopy as described in Methods. All images were captured with a 40x objective lens. mEH was stained with Cy-5 (red stain) in (A) vehicle control and (B) DMBA-treated ovaries. Genomic DNA was stained with YOYO-1 (green stain). Combined images for staining of both DNA and mEH are shown in (C) vehicle control and (D) DMBA-treated ovaries. Magnification of (E) vehicle control and (F) DMBA-treated ovaries. Broken arrows indicate primordial follicles. Arrowheads indicate small primary follicles. Scale-bar = 25μM.